Geochemical Perspectives Letters

Massive sulfide Zn deposits in the Proterozoic did not require euxinia

J.M. Magnall, S.A. Gleeson, N. Hayward, A. Rocholl

Supplementary Information

The Supplementary Information includes:

- Geological Setting
- Methodology
- Table S-1
- Figures S-1 to S-5
- Supplementary Information References

Geological Setting

The Carpentaria Zn Province is located in northern Australia (Fig. S-1a). Clastic-dominant (CD-type) Zn-Pb sulfide deposits are hosted primarily within carbonaceous mudstones of Proterozoic age in the Mt Isa – McArthur Basin. The Teena and McArthur River deposits occur within the Barney Creek Formation (BCF), which represents the peak transgressive phase of the River Supersequence depositional cycle (Page *et al*., 2000). The age of the Barney Creek Formation is constrained by U-Pb geochronology of zircons from the underlying Teena Dolostone (1639 ± 6 Ma) and the overlying Lynott Formation (1636 ± 4 Ma; Page *et al*., 2000). Zircons from volcaniclastic units within central BCF provide constraints of 1638 ±7 Ma, 1639 ± 3 Ma, and 1640 ± 3 Ma (Page and Sweet, 1998).

The sedimentary units of the BCF are regionally subdivided into the lower W-Fold Shale and overlying HYC Pyritic Shale members (Jackson *et al*., 1987; Pietsch *et al*., 1991). In the Teena sub-basin, the HYC Pyritic Shale members are sub-divided into the Lower, Middle and Upper members. At the McArthur River deposit, the sulfide mineralisation is located within the Lower HYC unit, which comprises variably dolomitic, silty carbonaceous mudstones, and is considered to be the deepest-water facies (Ireland *et al*., 2004; McGoldrick *et al*., 2010). The Teena deposit is also hosted within correlative stratigraphy of the Lower HYC, approximately 8 km away (see Fig. S-1b).

Both the W-fold Shale and HYC units preserve exhibit wedge-shaped geometries with abrupt thickening proximal to syndepositional growth faults (*e.g.*, McGoldrick *et al*., 2010; Kunzmann *et al*. 2019). Pronounced lateral lithofacies variations and local unconformities that indicate a change in depositional setting from a carbonate-dominated stable shallow marine platform, to a compartmentalized basin with numerous sub-basins and local paleo-highs associated with the onset of syndepositional extensional faulting and a marine transgression (McGoldrick *et al*., 2010). Some of the thickest parts of the Barney Creek depositional cycle occur within the Hot Spring-Emu sub-basin (Fig. S-1b), which hosts the McArthur River deposit in the northeast corner, and the

Teena deposit further west along the Bald Hills Fault.

There are 2 maximum flooding surfaces (MFS) within the Barney Creek Formation, recognisable from the high pyrite and organic carbon content, and which can be correlated across the entire McArthur Basin (Kunzmann *et al*., 2019). In the Teena sub-basin, the MFS intervals overly sequences of lesser pyritic mudstones that also contain a peak in carbonate (Fig. 1). We interpret this carbonate peak as being associated with reduced sedimentation rates during marine transgressions, thereby leading to the increased residence time of individual sedimentary packages within early diagenesis and corresponding higher levels of carbonate cementation (Taylor *et al*., 1995).

Following the development of their sequence stratigraphic framework, Kunzmann *et al*. (2019) suggested that sulfide mineralisation (with McArthur River used as an example) is likely associated with the development of these MFS intervals, owing to the high levels of sulfide and organic carbon. Notably, the sulfide mineralisation in the Teena sub-basin is actually located beneath the B1 MFS interval, and not within an obvious MFS interval. For example, there is a strong lateral decrease in pyrite abundance within the mineralised horizon, which for samples from TNDD015 drops to the levels observed within the Middle and Upper HYC units (termed Undifferentiated Barney Creek by Kunzmann *et al*., 2019). We would argue, therefore, that the mineralisation in the Teena sub-basin does not coincide with a MFS interval, as is frequently suggested for these deposits.

Methodology

A total of 3 mounts were prepared (one for each drill-hole), containing sub-sample pucks from 17 samples and multiple grains of the S0302A standard ($\delta^{34}S$ = 0.2 +/- 0.2 ‰; Magnall *et al*., 2016). Each mount was coated with Au and imaged using scanning electron microscopy (SEM; GFZ Potsdam). Sulfur isotope analyses were produced using a Cameca 1280-HR Secondary Ion Mass Spectrometer (SIMS) at the Helmholtz Zentrum (Potsdam). The primary beam (20 KeV $^{133}C^+$) was focused to a beam diameter of 5 µm. Simultaneous analysis of the isotopes of interest (^{32}S and ^{34}S) was conducted following the extraction of negatively charged secondary ions into Faraday Cups. The accuracy and precision of the data were monitored through the analysis of the standard, in duplicate, every 10 analyses. Time-dependent instrumental mass fractionation was determined for each analytical session and corrected for. Final uncertainties were between 0.2 and 1.0 ‰ (2σ) for each analysis.

Sulfide abundances were calculated on the basis of whole rock geochemical analyses of drill-core samples (Magnall *et al*., in prep.). Quarter core samples were sent for major element and assay (Cu, Pb, Zn) analysis with Bureau Veritas (Mt Isa) using oxidative fusion followed by XRF analysis.

As the only sulfide phases present are pyrite (FeS_2), sphalerite (ZnS) and galena (PbS), pyrite (mol/kg) was calculated as S_pyrite(mol/kg) = S_mol/kg – (Zn_mol/kg + Pb_mol/kg). A 1:1 correlation between Ca and Mg means that Ca_mol/kg provides a reliable approximation of total dolomite $CaMg[CO_3]_2$.

Supplementary Tables

Table S-1 Sulfur isotope data for SIMS analyses of pyrite at the Teena deposit. Data are described by lithological unit, paragenesis, and the dominant mineral assemblage within the individual sample puck that was extracted from the hand sample (*e.g.,* mudstone matrix, dolomite nodule *etc.*).

Table S-1 is available for download at http://www.geochemicalperspectivesletters.org/article2008.

Supplementary Figures

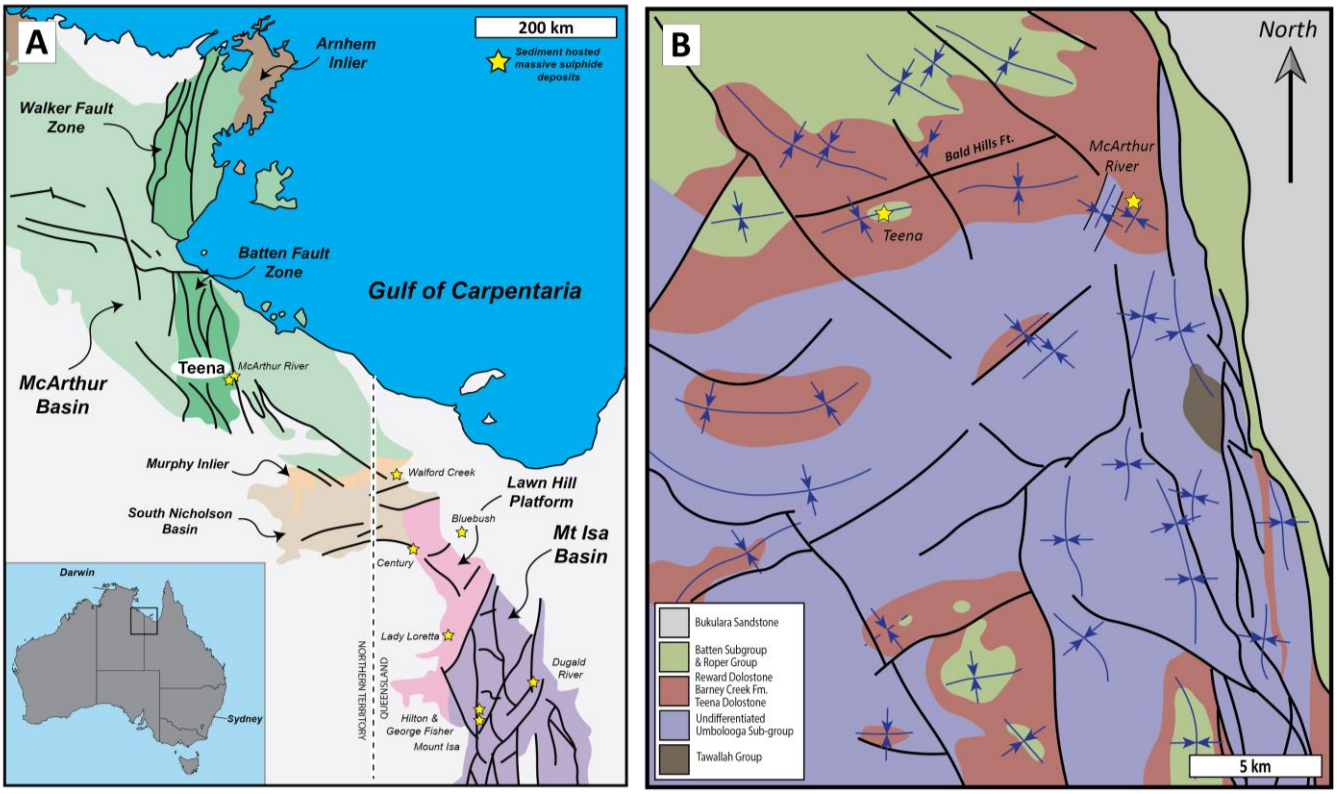

Figure S-1 **(a)** Map showing the geographical extent of the McArthur – Mt Isa basin and the locations of CD-type deposits (denoted by stars). **(b)** Sub-basins within the Emu-Hot Springs sub-basin. Both figures modified from McGoldrick *et al*. (2010).

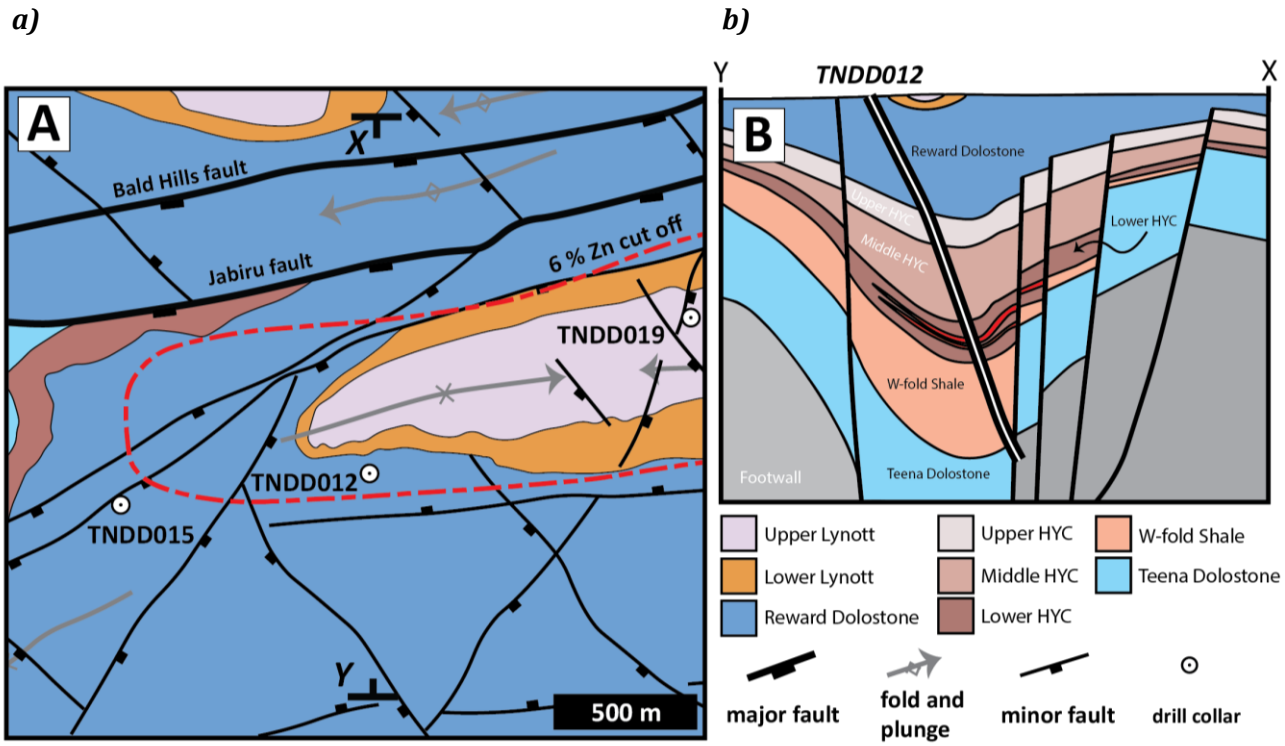

Figure S-2 **(a)** interpreted plan view geological map of the Teena sub-basin showing the main lithologies, geological structures (faults, folds) and drill-hole collars. **(b)** Schematic cross-section through the Teena sub-basin. Sulfide mineralistion occurs within the Lower HYC unit, and is coloured red.

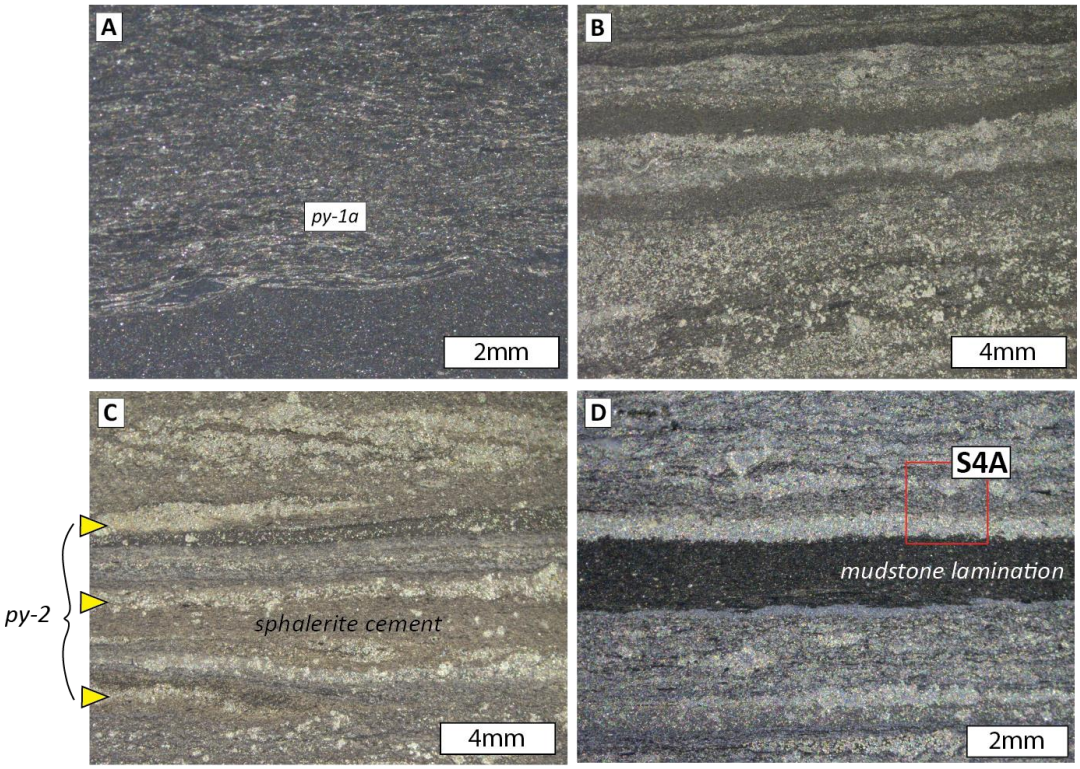

Figure S-3 Binocular microscope photographs of pre-ore and ore stage sulfide mineralisation from drill-core hand samples. **(a)** Discontinuous wispy aggregates of Py-1a within a carbonaceous mudstone sample from the maximum flooding surface high pyrite abundance interval in the upper HYC. **(b)** Stratiform aggregates of Py-2 with weak sphalerite cement mineralisation in the lower HYC mineralised interval. **(c)** Strong sphalerite cement mineralisation in the lower HYC mineralised interval. **(d)** Sharp contact between un-mineralised mudstone lamination and sphalerite and galena cement mineralisation within the lower HYC mineralised interval.

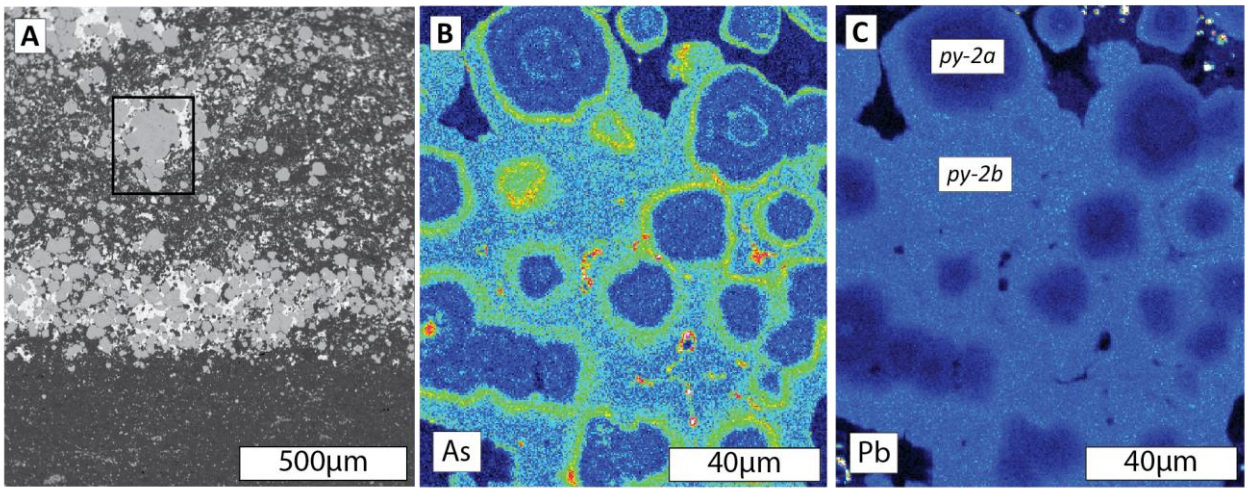

Figure S-4 **(a)** Backscatter electron (BSE) image of the interface between the mudstone lamination in **Figure S-2d** and ore stage sulfide cement mineralisation within the overlying stratiform pyrite. **(b)** Energy dispersive X-ray (EDX) mapping of As distribution within a zoned aggregate of Py-2. **(c)** EDX mapping of Pb distribution within a zoned aggregate of Py-2.

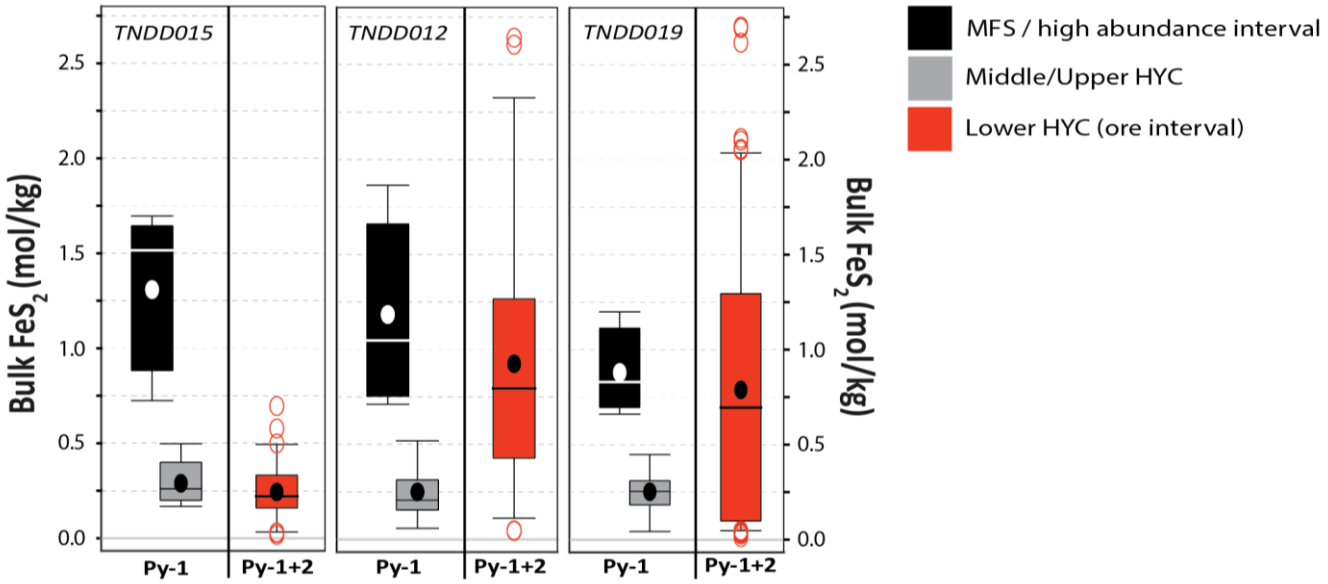

Figure S-5 Box and whisker plots for pyrite abundance (mol/kg; calculated from bulk rock) through the Lower and Middle HYC units of the Barney Creek Formation. The mineralisation is located within the Lower HYC unit, and there is clear lateral zonation in pyrite abundance from drill hole TNDD015 (un-mineralised) to TNDD012 (moderately mineralised) to TNDD019 (strongly mineralised). The high abundance pyrite interval located within the maximum flooding surface (MFS; black) has been separated from the rest of the Middle HYC (grey). Whereas the Middle and Upper HYC units contain primarily Py-1, the Lower HYC mineralised interval contains a mixture of Py-1 and Py-2 (predominantly Py-2 within TNDD019 and TNDD012).

Supplementary Information References

Ireland, T., Large, R.R., McGoldrick, P., Blake, M. (2004) Spatial Distribution Patterns of Sulfur Isotopes, Nodular Carbonate, and Ore Textures in the McArthur River (HYC) Zn-Pb-Ag Deposit, Northern Territory, Australia. *Economic Geology* 99, 1687–1709.

Jackson, M.J., Muir, M.D., Plumb, K.A., Jackson M.J. (1987) Geology of the southern McArthur Basin, Northern Territory (Australia). *Bulletin - Bureau of Mineral Resources, Geology & Geophysics, Australia*, 220.

Kunzmann, M., Schmid, S., Blaikie, T.N., Halverson, G.P. (2019) Facies analysis, sequence stratigraphy, and carbon isotope chemostratigraphy of a classic Zn-Pb host succession: The Proterozoic middle McArthur Group, McArthur Basin, Australia. *Ore Geology Reviews* 106, 150-175.

Magnall, J.M., Gleeson, S.A., Stern, R.A., Newton, R.J., Poulton, S.W., Paradis, S. (2016) Open system sulphate reduction in a diagenetic environment - Isotopic analysis of barite ($\delta^{34}S$ and $\delta^{18}O$) and pyrite ($\delta^{34}S$) from the Tom and Jason Late Devonian Zn-Pb-Ba deposits, Selwyn Basin, Canada. *Geochimica Cosmochimica Acta* 180, 146–163.

McGoldrick, P., Winefield, P., Bull, S., Selley, D., Scott, R. (2010) Sequences, Synsedimentary Structures, and Sub-Basins: the Where and When of SEDEX Zinc Systems in the Southern McArthur Basin, Australia. *Economic Geology Special Publication* 15, 367–389.

Page, R.W., Sweet, I.P. (1998) Geochronology of basin phases in the western Mt Isa Inlier, and correlation with the McArthur Basin. *Australian Journal of Earth Sciences* 45, 219-232.

Page, R.W., Jackson, M.J., Krassay, A.A. (2000) Constraining sequence stratigraphy in north Australian basins: SHRIMP U-Pb zircon geochronology between Mt Isa and McArthur River. *Australian Journal of Earth Sciences* 47, 431–459.

Pietsch, B.A., Rawlings, D.J., Creaser, P.M., Kruse, P.D., Ahmad, M., Ferenczi, P.A., Findhammer, T.L.R. (1991) 1:250,000 Geological Map Series Explanatory Notes, Bauhinia Downs SE53-3.

Taylor, K.G., Gawthorpe, R.L., Van Wagoner, J.C. (1995) Stratigraphic control on laterally persistent cementation, Book Cliffs, Utah. *Journal of the Geological Society London* 152, 225–228.